Quantitative Fractography of Profiles By Digital Image Processing: Analysis Of Ti-4Al-4V at Different Microstructural Conditions

Ana Lúcia Horovistiz[1], Luciano M. F. Ribeiro[1], Kamila A. Campos[1], Glaucio A. Jesuino[1], Luis Rogerio de O. Hein[1]*
Short-running Title: QUANTITATIVE FRACTOGRAPHY BY IMAGE PROCESSING
[1]Laboratório de Análise de Imagens de Materiais (LAIMat), Departamento de Materiais e Tecnologia (DMT) UNESP - Campus de Guaratinguetá
Av: Dr. Ariberto Pereira da Cunha,333, Pedregulho, Guaratinguetá-SP,CEP 12516-410,Phone (12) 525-2800 - 248, Fax: (12)525-2466. E-mail :rhein@feg.unesp.br

Abstract

This work is an example of the improvement of quantitative fractography by means of digital image processing and light microscopy. Two techniques are presented to investigate the quantitative fracture behavior of Ti-4Al-4V heat-treated alloy specimens, under Charpy impact testing. The first technique is the Minkowski method for fractal dimension measurement from surface profiles, revealing the multifractal character of Ti-4Al-4V fracture. It was not observed a clear positive correlation of fractal values against Charpy energies for Ti-4Al-4V alloy specimens, due to their ductility, microstructural heterogeneities and the dynamic loading characteristics at the region near the V-notch. The second technique reconstruct the fracture surface image, extracting in-focus regions for each picture from a stack of images acquired at successive focus positions, computing the surface roughness. The extended-focus reconstruction was used to explain the behavior along fracture surface. Ti-4Al-4V is the product of recycling the Ti-6Al-4V alloy by double fusion in electron beam furnace.

Keywords: image processing, fractal analysis, quantitative fractography, extended-focus reconstruction, titanium alloys

Introduction

The concept of fractal geometry arose due to necessity of to characterize, explain, and model complex objects (rough and discontinuous) which cannot be described by Euclidean geometry.
In fractal theory, an irregular geometry is considered a transition between two regular ones. A fractal curve for instance, the Koch flake, has a fractal dimension, D, between a straight line and a plane ($1 < D < 2$), in the same way, the fractal dimension of a surface varies between 2 and 3. Thus, the dimension increases as the tortuosity increases.
Other characteristic attributed to fractal structure is the self-similarity, which can be defined as invariant about the geometric properties of an object, under isotropic rescaling of its length (1). Or, as defined by Russ (2), a rugose object whose rugosities show up at any length scale.
The use of fractal dimension in the field of materials science is recent and was developed after the work of Mandelbrot (1), which introduced the fractal concept. Mandelbrot and collaborators studied the fracture surfaces of 300-grade maraging steel and correlated the fractal dimension, obtained by Slit Island analysis, with the impact energy (3).
Since then, most of researchers agree that fracture surface is a fractal because it presents self-similarity. Thus, this kind of surface is often studied by fractal dimension in order to develop solid correlations between microstructure and mechanical properties.
In the present paper, standard V-notch Charpy specimens were used in order to establish a correlation between the fractal dimension and the impact energy. The vertical sectioning method was applied to obtain the fracture profiles and the fractal dimension was calculated by means of the Minkowski method (2).
The material was the Ti-4Al-4V alloy, obtained by the recycling of Ti-6Al-4V scraps. This recycling involves double-fusion in electron beam furnace, occurring the reduction in Aluminum content during fusion process.

Materials and Methods

The Ti-4Al-4V (or Ti-4-4) as-cast samples were heat treated in box furnace to four conditions. These heat treatment procedures can be described as following:

As-cast;
Heating at 900°C, with rate heating of 10°C/min, stay by 30min and subsequent water cooling, with two cycles;

3. Heating at 900°C, with rate heating of 10°C/min, stay by 30min and subsequent water cooling, with four cycles;
4. Heating at 950°C, with rate heating of 30°C/min, stay by 30min and subsequent water-cooling.

Impact testing was realized at room temperature. The absorbed energies were measured to the four conditions, according to table 1. Five specimens for each condition were tested. Among these, one specimen for each condition was randomly selected for fractal analysis.

Table 1: Impact energy values of Ti-4Al-4V

Specimen	Impact energy of selected specimen (N.m)	Mean and standard deviation (N.m)
1	54.0	50.7 ± 2.32
2	20.6	22.0 ± 3.80
3	20.6	28.2 ± 5.45
4	30.4	29.7 ± 4.83

Metallography

The metallography consisted on to cover the fractured specimens with epoxy resin in order to preserve the surface details, before sectioning. The cutting in a precision saw was done along a plain orthogonal to fracture surface, containing both the V-notch and the end of fracture. The specimens were then mounted in phenolic resin for low deformation mechanical polishing.
Five fracture profiles were obtained by vertical section method for each sample. This technique consists on successive polishing steps to reveal the vertical section through the fractured surfaces.
The equipment used for image acquisition, processing and analysis includes a Nikon Epiphot 200 light microscope, a Pixera 120 ES digital camera, Scion Image Beta 4b and UTHSCSA Image Tool 2.0 alpha 2 software with Reindeer Games Image Processing ToolKit 3.0 (IPTK) plug-ins, respectively. The images were captured with 200x magnification under brightfield contrast and 640x480 pixels of spatial resolution, according to Fig. 1.

Image Processing and Analysis

a) Pre processing

The image processing first involved the thresholding for binarization in the original image, observing the profile integrity. The IPTK Fill Hole filter was applied to close holes after binarization, mainly occurring due to inclusions or precipitates in matrix or heterogeneities in mounting resin. Figure 2 shows the image after Fill Hole filter.

Figure 1. Profile polished of the fractured surface near to Charpy V-notch region.

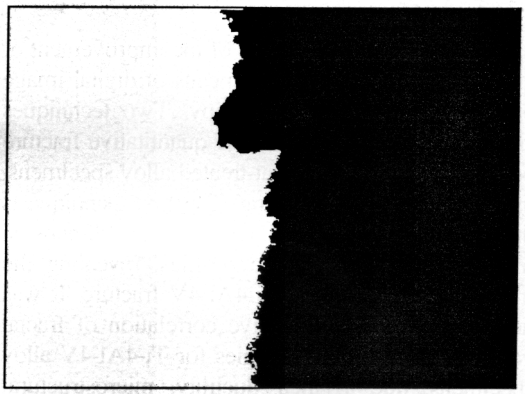

Figure 2. Fracture profile in Figure 1 after Fill Hole filter

b) Fractal Routine using Minkowski Method

The Minkowski method consists on the use of a series of erosions and dilations, morphological operations that remove and add pixels, respectively, throughout the binary profile. Dilation adds any background pixels that touch the features, while erosion removes any feature pixels that touch the background. A Minkowski's sausage is obtained by sequences of dilation, Figure 3a, followed by erosion, Figure 3b, and XOR operation (Boolean operation that can be produced by a sequence of AND, OR and NOT), Figure 3c.
The routine stores the values of increments and perimeters of sausages (effective area divided by length and number of cycles) into the two arrays. The values were plotted and two line segments were found.
The result is an agreement on the Kaye's concept about multifractal profiles (4). The line segments have two different slopes: a structural region, that is comprised at large scales and has a major value, and the textural region, which emerges at fine scales.
The structural dimension corresponds at major slope and describes one physical process that controls the surface topography, such as the local microstructure, while the minor scale is the textural, and is related to the overall fracture process.

This macro routine was developed under Scion Image Beta 4b, based on NIH Image for MacOS, modified for MS Windows 95/98/NT by Scion Corporation. The table 2 shows the fractal data measured for all profiles.

Table 2. Fractal dimension values

Samples	Structural D_f	Textural D_f
1	1.16	1.15
	1.26	1.20
	1.17	1.12
	1.22	1.15
2	1.15	1.13
	1.04	1.10
	1.18	1.13
	1.17	1.15
3	1.08	1.11
	1.09	1.08
	1.13	1.09
	1.22	1.16
4	1.20	1.15
	1.13	1.12
	1.07	1.10
	1.11	1.10

Results and Discussion

It was expected a positive relation between the fractal dimension of fracture profile and the impact toughness, as observed for a micro-alloyed steel by present authors (5). In general, the morphology of fracture surface can be related to the material properties, so that, materials that present a large toughness have a higher plasticity which, in turn, must be associated with a rough surface and consequently a high fractal number (2). In this paper, however, the curves of fractal dimension values against impact energies did not present a significant growth tendency, as showed in the Figure 4.

The as-cast Ti-4Al-4V presents a heterogeneous microstructure with α-lamellae phase colonies distributed with different orientations into β matrix, that Markovsky (6) attribute to own mean mechanical properties. Rapid heat treatment can improve mechanical properties by cycles of heating and quenching promoting the refinement of intragrain structure due to martensitic reactions (7).

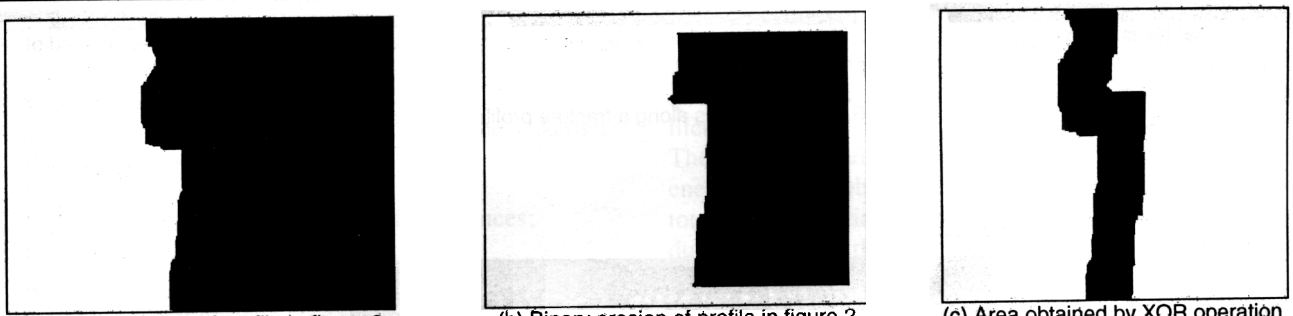

(a) Binary dilation of profile in figure 2 (b) Binary erosion of profile in figure 2 (c) Area obtained by XOR operation

Figure 3. Erosion/ dilation steps for Minkowski fractal dimension measurement

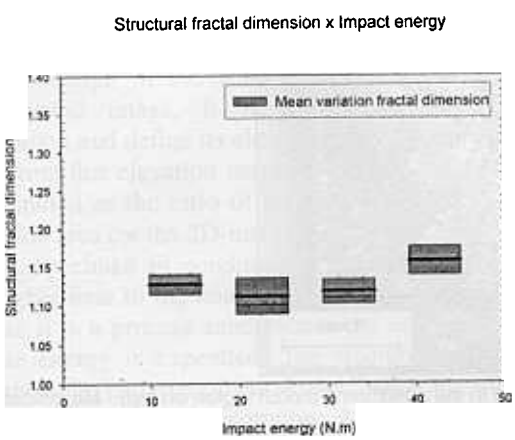

Figure 4 (a). Textural fractal dimension

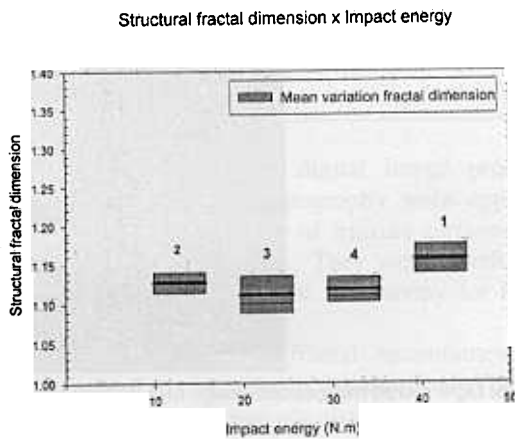

Figure 4 (b). Structural Fractal Dimension

For example, the microstructure after heat treatment at 950°C exhibits martensitic α, α-lamellae and β morphologies as show the Figure 5 (a, b, and c). The fracture process during impact test is strongly changed throughout the specimen surface due to the heterogeneity of Ti-4Al-4V alloy and the evolution of stress distribution during dynamic loading. Furthermore, there are several changes in fracture path, due to different fracture mechanisms, as showed in Figure 6. These changes of mechanism reflect on topography producing surface roughness variation (Figure 7). It must have a significant influence on the fractal dimension results.

Figures 7a, 7b and 7c show extended-focus reconstructions from stacks of light micrographs. These reconstructions were done to measure the surface roughness of each region. The basic idea to extend the depth of field of optical microscopes is to extract the in-focus region from each picture in the stack. The images in each stack were pictured at different focus positions, by moving the objective lens with a constant pitch of 2μm, that is equivalent to the focus range of the 20X objective. It is well known that in-focus regions contain high frequencies (8), due to contours, patterns and edges.

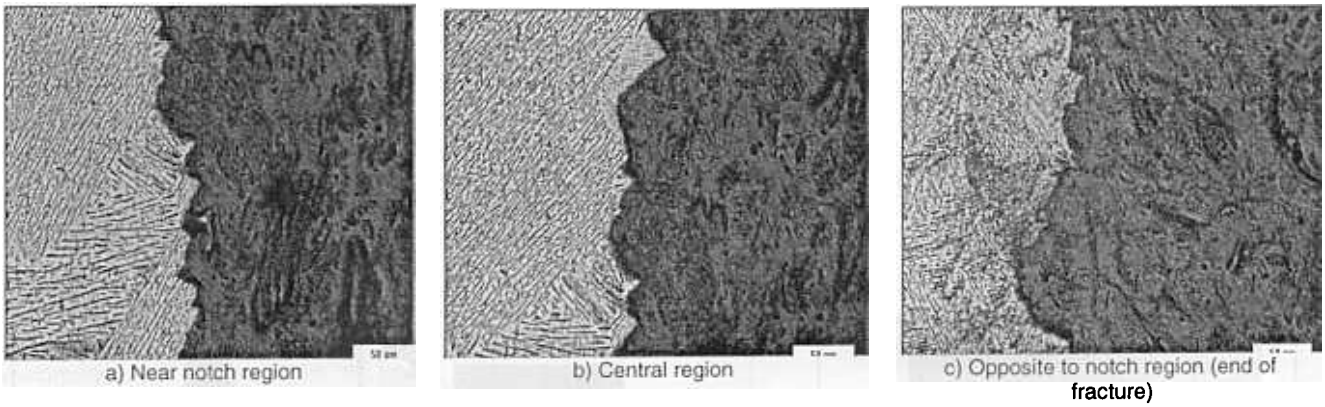

Figure 5. Microstructures along a fracture profile (condition 4).

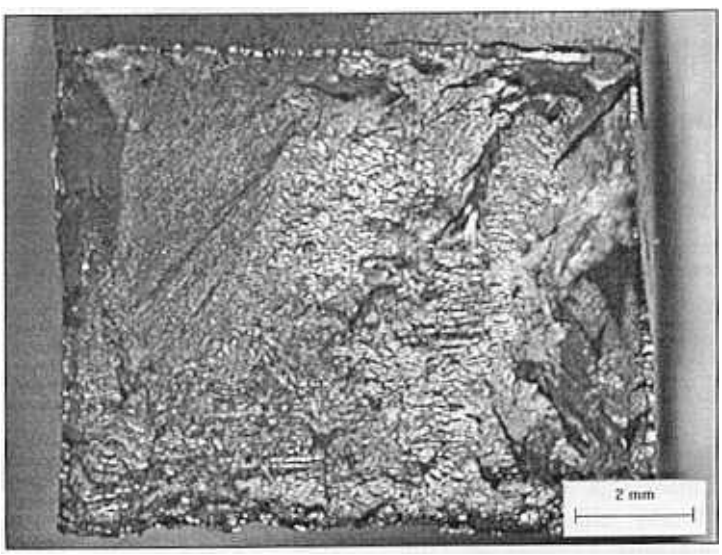

Figure 6. Light stereo microscope image of a general view of the fracture surface in the condition 4 (notch region on top). Magnification: 13.4 X.

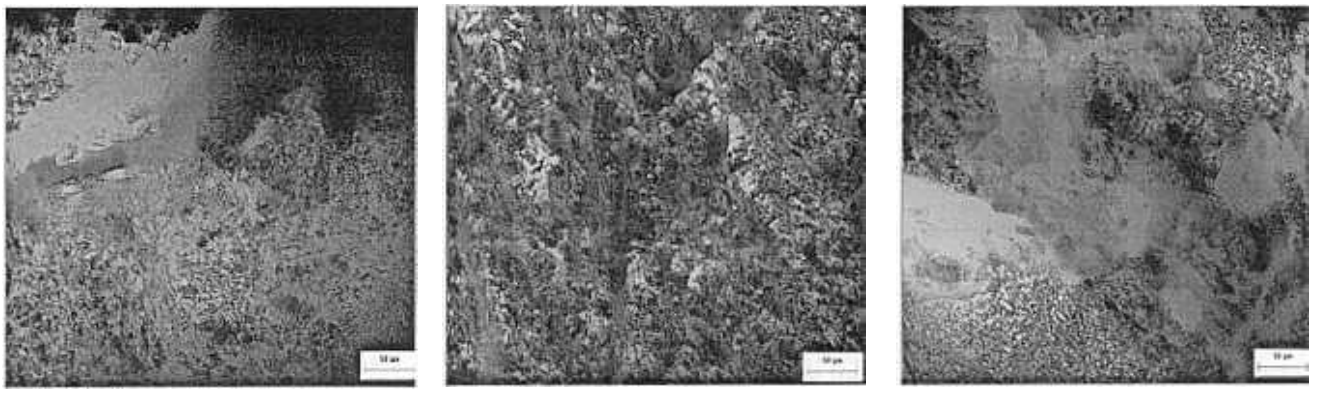

a) Near notch region
(R_S = 7544.3, FR = 386 µm)

b) Central region
(R_S = 986.30, FR= 142 µm)

c) Opposite to notch region
(R_S = 508.02, FR= 190 µm)

Figure 7. Extended-focus reconstructions of fracture surface from light microscope with 200x magnification and 848x640 resolution. FR means the focus range, or the total travel distance of objective lens to focus all surface regions.

In this way, a high-pass filter must be applied to extract in-focus areas from each image on stack and then the maximum for each pixel position through the stack is selected to reconstruct the extended-focus image. In this paper, it is proposed a sequence of rank and convolution filters that was applied to filter high frequencies regions from the dark-field images:

a) a median filter, to reduce noise;
b) a light high-pass filter, with the kernel
$$\begin{bmatrix} -1/9 & -1/9 & -1/9 \\ -1/9 & 8/9 & -1/9 \\ -1/9 & -1/9 & -1/9 \end{bmatrix}$$ to increase small differences;
c) a stronger high-pass filter, using the kernel
$$\begin{bmatrix} -1 & -1 & -1 \\ -1 & 9 & -1 \\ -1 & -1 & -1 \end{bmatrix}$$ to delineate high frequency patterns

As each image in the stack contributes for the final reconstructed image, it is possible to separate its contribution and define its elevation, building an elevation map. From this elevation map, the surface roughness can be computed as the ratio of the true surface area by the projection area (or the 2D-image area).

For the specimen in condition 4, the surface roughness was higher near to the notch (Figure 7a). It was expected because it is a process zone, where the major amount of fracture energy is expended. The fracture in Figure 7a presents some patterns of intralamellae tearing and some facets of intergranular separation. At the central region (figure 7b), the fracture path is clearly intragranular, suggesting interlamelae separation, also observed in figure 5b. It results on the lower measured focus range, also expected due to the relatively stable crack propagation. Finally, it can be observed a rough pattern in figure 7c, with intergranular sliding facets, reducing surface roughness, and some large dimples, denoting the ductile rupture mechanism under the plane stress field.

These results can explain the unclear tendency for the fractal values against Charpy energies. Maybe, in this case, the measurement of fractal values could be more effective if done at central region instead of near to V-notch, because its more regular behavior. In fact, this question remains unsolved and is not well studied in the literature.

The best correlations between fractal values and impact energies were observed for cleavage fractures or low toughness materials (3; 9; 10). The process zone for ductile materials does not present a regular behavior along width, as observed by Horovistiz (11) for Al 7050 alloy, introducing disparities in the correlation of fractal values against fracture energies. The low energy in fragile fracture minimizes the intensities of elevation changes in process zone, resulting in more regular profile patterns for fractal measurements.

Conclusions

In this work, two different digital image processing solutions for quantitative fractography were applied to study the topographic behavior of fracture surfaces of Ti-4Al-4V under impact loading. They were developed to improve the capabilities of light microscopy for fracture analysis.

The Minkowski method for fractal measurement from profiles permitted to characterize the multifractal behavior of the fracture surface. It was not observed a clear positive correlation between fractal values and Charpy energies for Ti-4Al-4V alloy specimens, due to their ductility, microstructural heterogeneities and the dynamic loading characteristics at process zone.

The extended-focus reconstruction was used to explain the behavior along fracture surface, using a light microscope to measure local values of surface roughness. The changes in fracture mechanisms are reflected by the local surface roughness data, being the region near Charpy notch the most irregular.

Acknowledgments

This work has been supported by FAPESP (Fundação de Amparo à Pesquisa do Estado de São Paulo) under grant number 1997/6287-5. The authors acknowledge the Foundation for this support.

References

1. Mandelbrot, B.B. (1983) The fractal geometry of nature, W.H. Freeman, New York, 468 p.
2. Russ, J.C. (1994) Fractal surfaces. Plenum Press, New York, 309p
3. Mandelbrot, B.B., Passoja, D.E., Paullay, A.J. (1984) Nature, 308:721-722
4. Kaye, B. H. (1989) Image analysis techniques for characterizing fractal structures. The fractal approach to heterogeneous chemistry, John Wiley & Sons, New York, p. 55-66
5. Campos, K.A., Horovistiz, A.L. Roza, J.E. Pereira, M.S Hein L.R.O. (2000) Acta Microscópica, to be published.
6. Markovsky, P.E. (1995) Materials Science and Engineering A, 190: L9-L12.
7. Ivasishin, O.M. (1999) Materials Science and Engineering A., 142-154
8. Kaneda, K., Ishida, S., Ishida, A., Nakamae, E. (1992) The Visual Computer, 8:351-360
9. Charkaluk, E. Bigerelle, M. Iost, A. (1998) Engineering Fracture Mechanics. 61:119-139
10. Hilders, O.A., Pilo, D. (1997) Materials Characterization 38:121-127
11. Horovistiz, A.L.(2000) Técnicas e parâmetros para análise de perfis na fractografia quantitativa, Master thesis, UNESP, Guaratinguetá, 141 p.